Energy Conversion and Management: X 19 (2023) 100384

Contents lists available at ScienceDirect

Energy Conversion and Management: X

journal homepage: www.sciencedirect.com/journal/energy-conversion-and-management-x

Estimation of generator electrical power output and turbine torque in modelling and field testing of OWC wave energy converters

A.A.D. Carrelhas [a], L.M.C. Gato [a,*], J.C.C. Henriques [a], G.D. Marques [b]

[a] IDMEC, Instituto Superior Técnico, Universidade de Lisboa, Av.Rovisco Pais 1, 1049-001 Lisboa, Portugal
[b] INESC-ID, Instituto Superior Técnico, Universidade de Lisboa, Av. Rovisco Pais 1, 1049-001 Lisboa, Portugal

ARTICLE INFO

Keywords:
Generator efficiency
Wave-to-wire model
Field testing
Oscillating water column
Wave energy

ABSTRACT

The oscillating water column is one of the most tested and used wave energy converter types. It requires the use of an air turbine connected to an electrical generator. The deep understanding of all physical quantities of the energy chain components is based on transducers. The electrical generator efficiency is a key input to wave-to-wire numerical models for wave energy conversion to enable the industry to embark on projects with reliable data. Assembly of a standard torque meter is not feasible in prototypes following an industrial design. Therefore, the turbine shaft power must be calculated from the electrical generator dry-testing results at various rotational speeds and loads. This paper presents normalised data for estimating generator power output and turbine torque based on generator efficiency measurements. Experimental results show the electrical generator efficiency dependency on the rotational speed and load. A new kind of filter to post-process the raw data was used. The results will be used as a reference for wave-to-wire numerical models of oscillating water columns and post-processing the data from prototypes operating in real sea state conditions.

1. Introduction

Given the steady increase in global energy demand and the urgency to meet the goals of the Paris Agreement, there is a need to transform the global energy system and achieve full decarbonisation between 2055 and 2080 [1]. Moreover, recent events have triggered the rise and volatility of energy commodity prices such as crude oil or natural gas. Energy independence and energy security are common goals around the world [2]. As a result, the energy transition has taken off, and renewable energy technologies are more sought after than ever. Renewable energy sources are central to the implementation of this transition [3] because of their environmental and economic benefits.

Wave energy is a renewable form whose power density is expressive in territories facing the ocean and can be predicted days in advance. There are different types of wave energy converters (WECs). Most WECs use the motion of ocean waves to generate electricity. Various physical mechanisms for extracting energy from the waves lead to different power take-off (PTO) systems concepts. In addition, the device may also have other configurations in terms of its structure and location. They can be categorised according to their principle of operation: oscillating water column (OWC) [4], oscillating body [5], over-topping [6] and membrane-pump [7]. For a comprehensive overview and comparison, see Ref. [8].

The OWC device distinguishes itself from the other concepts due to its inherent simplicity in construction and reliability since the only moving part is a turbine generator set located above the water-column free surface. It consists of a hollow structure open below the water-free surface with an air chamber above the free surface. The natural movement of the waves forces the water column to compress and expand the air inside the pneumatic chamber. There is a hole in the top of the air chamber where an air turbine generator set is installed. Compression and suction create airflow through the turbine coupled with an electrical generator that causes it to rotate and produce electricity. The OWC WEC type already has several prototypes operated in real conditions: either of the fixed type (e.g., Pico wave power plant [9], Limpet [10], Mutriku wave power plant [11]) or floating type (IDOM MARMOK A-5 [12], OE35 Buoy [13], UniWave 200 [14]) OWCs. Two recent prototypes were tested in real sea conditions equipped with a 30 kW biradial turbine with fixed guide vanes [15] within the European project H2020 OPERA [16]. First in the Mutriku wave power plant integrated into the breakwater and later in the floating MARMOK-A-5 OWC device at the BiMEP test site.

The path from the concept of the OWC to its use under real

* Corresponding author.
E-mail addresses: ana.carrelhas@tecnico.ulisboa.pt (A.A.D. Carrelhas), luis.gato@tecnico.ulisboa.pt (L.M.C. Gato), joaochenriques@tecnico.ulisboa.pt (J.C.C. Henriques), gil.marques@tecnico.ulisboa.pt (G.D. Marques).

https://doi.org/10.1016/j.ecmx.2023.100384

Available online 28 April 2023

Nomenclature

Romans

i	Current [A]
I	Inertia [kg m^2]
P	Power [W, VA]
t	Time [s]
T	Torque [Nm]
u	Voltage [V]

Greek symbols

η	Efficiency [–]
Ω	Rotational speed [rad/s]

Superscripts

rated	Rated value

Subscripts

12	Line 1 to line 2
23	Line 2 to line 3
1	Line 1
3	Line 3
gen	Generator
motor	Motor
turb	Turbine

Acronyms

AC	Alternating Current
OWC	Oscillating Water Column
PTO	Power Take-Off
PWM	Pulse Width Modulation
SG	Savitzky-Golay
VFD	Variable Frequency Drive
WEC	Wave Energy Converter

conditions follows the typical engineering approach [17]: (1) concept; (2) wave-to-wire numerical modelling; (3) model tests in dry test rigs; and (4) experimental campaign under real conditions. A problem in estimating two critical variables in steps 2 and 4 was identified as a research gap: *How to calculate the generator electrical power output and turbine torque in wave-to-wire numerical models and prototypes, respectively?* The following two paragraphs explain the problem for each step.

As for step 2, preparation must be done before deployment using powerful numerical models replicating the system's behaviour under the variable flow conditions in an OWC. The wave-to-wire models help predict all the components' behaviour and performance to have more reliable and less risky projects. The generator's electrical power output is usually calculated from the turbine's shaft power output requiring the knowledge of the generator's efficiency from the mechanical energy supplied by the turbine to the generator [18–20]. Wave-to-wire models usually assume the generator's efficiency as a single curve as a function of the load, independent of the rotational speed [21–23], as provided by the machine manufacturers. This information is supplied for the nominal rotational speed, and the air turbines for OWC devices operate at a variable rotational speed. Therefore, a complete efficiency map showing the performance for different rotational speeds and loads is required. This directly affects the estimation of all decision variables derived from these models.

In what concerns step 4, the prototype is deployed into real sea state conditions. Five main variables must be correctly measured in assessing the air turbine performance: the pressure head, flow rate and air density to calculate the available power, and the rotational speed and turbine torque to calculate the shaft power produced. Except for the torque, all variables may be measured with pressure transducers, temperature sensors and encoders. A torque meter may be assembled between the turbine's rotor and the generator in scaled models placed on well-balanced test benches, with good access to all the components. In a prototype, this sensor should not be mounted into a turbine generator set due to its fragility. Therefore, a method to determine the turbine torque is essential for developing this component.

This paper presents a method for estimating generator electrical power output and turbine torque in two important phases of an OWC WEC development: i) numerical modelling and ii) experimental campaigns with prototypes in the laboratory or at sea, respectively. The efficiency of an electric generator is evaluated in a dry test rig with two electric machines mounted in the same shaft line. The classical torque estimation in squirrel cage induction machines can be performed using several other methods [24]. They are generally implemented using stator currents and the assessment of stator flux leakages. In this case, only the stator copper losses are considered. More recently, in Ref. [25], these methods were improved using the same principle but adding extra blocks to improve the estimation accuracy. The approach presented here for determining efficiency considers all losses in the electrical machine.

A detailed method of using the experimental data in the two applications mentioned above is shown. They have been deliberately normalised to the generator's rated power to be used easily. In addition, new filters based on Savitzky-Golay filters were developed for the pulse width modulation (PWM) signals.

The contributions of the paper are:

- Experimental mapping of the efficiency of a standard induction generator that can be used in OWC WECs.
- Development of a method to estimate the generator electrical power output from the calculated turbine shaft torque in wave-to-wire numerical models of OWC WECs.
- Development of a method to estimate turbine torque for OWC prototypes in field testing under real sea conditions.
- Development of a new type of filter for PWM-generated signals.

The structure of the paper is as follows. Section 2 describes the methods and materials used to determine electrical generator output in wave-to-wire models and turbine torque in prototypes under real sea state conditions. Section 3 presents the efficiency mapping results obtained for a 30 kVA generator. They are later used to determine coefficients of rational polynomial functions to estimate generator power output and turbine torque for the above applications. The coefficients are normalised to the rated power of the generator so that they can be used for other applications with different power ratings. The conclusion is presented in Section 4.

2. Methods and materials

As identified in Section 1, the generator efficiency at different rotational speeds and loads is required in numerical modelling or experimental campaigns of OWC WECs. Since the turbine-generator rotational speed and its loads vary greatly (due to the intrinsic wave resource that generates the oscillating pressure in the OWC pneumatic chamber), a generator's efficiency map with a large discretisation of both rotational speed and load is needed. A test rig was built to reproduce the PTO performance and obtain these data. Note that OWC PTO is a turbine generator set, and in the test rig, the turbine is replaced by a motor. The generator's efficiency can be measured for the given rotational speed of the assembly and applying a counter torque. This is done at constant rotational speed and different counter torque values. Then the rotational speed changes and different counter torques are tested again. The result is an efficiency map which can be interpolated by the user to calculate the generator's electrical power and turbine torque in numerical modelling and experimental campaigns.

The experimental apparatus and the methods used for the study are presented and discussed in the following sections.

2.1. Dynamics of the oscillating water column system

In an OWC device, the movement of the water-free surface in the pneumatic chamber causes an alternating airflow in the turbine rotor blades. Since the turbine is self-rectifying, this airflow will produce a one-way movement in the rotor, producing mechanical power. The turbine is directly coupled to a generator. When the turbine produces torque, the generator must apply counter torque to reach the rotational speed set by the turbine-generator controller. The counter torque must be such that the turbine generator operates at its best efficiency to maximise power generation.

The dynamics of the turbine and generator is derived from Newton's second law of motion as

$$I\frac{\mathrm{d}\Omega(t)}{\mathrm{d}t} = T_{\mathrm{turb}}(t) - T_{\mathrm{gen}}(t), \tag{1}$$

where I is the inertia of the rotating masses of the power take-off (turbine, generator and couplings), t is the time, T_{turb} is the turbine shaft torque, T_{gen} is the generator counter torque and Ω is the rotational speed. The relation between the electrical generator counter torque, T_{gen}, and the electrical power at output terminals, P_{gen}, is given by

$$T_{\mathrm{gen}} = \frac{P_{\mathrm{gen}}}{\Omega\eta_{\mathrm{gen}}}, \tag{2}$$

where η_{gen} is the electrical generator efficiency. Depending on whether a user performs calculations with wave-to-wire numerical models [23] or post-processes experimental data from prototype field campaigns [26] different variables are unknown from Eq. (1) and (2).

As far as the numerical models are concerned, it is a question of determining the electrical power output. The inertia is known. The turbine torque is calculated from the rotational speed and pressure using the turbine performance curves, and the generator counter torque is the torque calculated by the control algorithm. The generator counter torque and the rotational speed are then used to calculate the generator's efficiency, $\eta_{\mathrm{gen}}(T_{\mathrm{gen}},\Omega)$, to subsequently find the electrical power output from Eq. (2).

In the case of experimental post-processing data from prototypes, the unknown variable is the turbine torque. The inertia is known. The measurement of the generator's electrical power output and rotational speed is done with robust instruments easily available. With these two variables the efficiency of the generator is calculated $\eta_{\mathrm{gen}}(P_{\mathrm{gen}},\Omega)$ and subsequently the counter torque using Eq. (2). The turbine torque is then calculated from Eq. (1).

Therefore, determining the generator's efficiency for different rotational speeds and loads is paramount. Note that the load profile of a turbine generator set for OWC devices is variable due to the intrinsic nature of the flow that drives it.

2.2. Efficiency mapping: Experimental procedure

An experimental procedure was developed to determine the generator's efficiency at different loads and rotational speeds. In a test rig equipped with a torque meter, the generator is driven by an electric motor at a constant rotational speed for different values set by a variable frequency drive (VFD). Both machines were grid connected through a VFD. The one that controls the motor uses speed control to maintain the imposed rotational speed. The generator's VFD uses torque control with an encoder to set the prescribed counter torque.

The experimental procedure was as follows. The rotational speed was set by the motor's VFD and the torque by the generator's VFD. The torque and the rotational speed were set in opposite directions. For a given test with pair of variables $(\Omega, T_{\mathrm{gen}})$, the prescribed rotational speed Ω is the same during the test because the motor's VFD is being controlled in speed control. Since the generator's VFD is controlled in torque control with encoder it will impose the prescribe torque. For each pair of rotational speed and torque, voltage, current, torque and rotational speed measurements were performed and acquired by the data acquisition system. The acquired signals were then filtered following the method described in Section 2.5, and the calculations were performed following the procedure presented in Section 2.4. The rotational speed was varied in intervals of 100 rpm, between 100 and 2900 rpm.

The dynamics of this assembly follows Eq. (1) where T_{turb} is now T_{motor}. At steady state the rotational speed is constant ($\mathrm{d}\Omega(t) = 0$) and from Eq. (1), it is $T_{\mathrm{motor}} = T_{\mathrm{gen}}$. This result shows that the two machines apply an equal torque magnitude acting in different directions to maintain the set rotational speed. Note that this procedure is performed to determine the efficiency of the generator for a pair $(\Omega, T_{\mathrm{gen}})$. During simulation or operation in the real sea, the rotational speed varies greatly because the load profile of a turbine generator set for OWC devices is variable due to the intrinsic nature of the flow.

2.3. Efficiency mapping: Description of the apparatus

The electrical generator is a 480 V, 30 kVA four-pole squirrel-cage asynchronous machine. It is connected to the grid using a 37 kVA four-quadrant VFD allowing the electric machine to operate as a motor or generator.

The constructed rig for the experimental tests is schematically shown in Fig. 1. It consists mainly of the generator, the VFD that controls the generator, a 160 kW motor controlled by a second VFD, a torque meter connecting the generator and the electric motor via semi-rigid couplings, and current and voltage transducers at mains terminals. Four conductor cables connected the generator to the VFD and the VFD to the grid: three phases and ground. Fig. 2 shows photos from different perspectives of the test rig.

A total of six variables were measured: two line currents, two line-to-line voltages, the torque and rotational speed. Table 1 lists the instrumentation used for the experimental tests.

The current measurement was carried out with Hall effect current transducers. A calibration was performed with the simultaneous reading of the current measured by the sensor and by a calibrated ammeter, with a range of 0–50 A and an accuracy of 0.5% of the measured value.

Voltages were measured with Hall effect closed loop transducers. They were calibrated with a 0–120 A range voltmeter with an accuracy of 0.1% of reading. As with the previous instrument, the voltage readings from the voltmeter and the transducers were measured simultaneously.

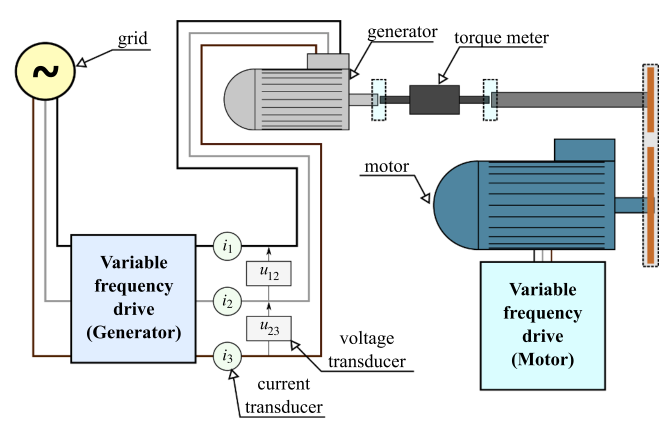

Fig. 1. Schematic representation of the test rig.

(a) (b) (c)

Fig. 2. Test rig views: (a) VFD of the generator and the current and voltage transducers; (b) top view of the generator with the torque meter; (c) test bench.

Table 1
List of the instrumentation used for the experimental testing. RV - Reading value.

Designation	Range	Accuracy
Ammeter	0–200 A	±1% RV
Voltmeter	0–500 V AC	±0.9% RV
Torque meter	±200 Nm	±0.5 Nm
Encoder	0–4000 rpm	±1/30 rpm

The torque was measured by a torque meter in-house calibrated with a mechanism based on the lever arm principle and a set of calibrated masses.

The rotational speed was measured with an encoder, the signal of which was input into the control unit of the generator's VFD. Then the signal was acquired at one of the analogue connections of the VFD control unit.

The data acquisition system consisted of two data analogue-to-digital boards and a Matlab session-based interface routine to read and process the signals from the transducers. One of the acquisition boards had read the voltage and current signals, and the second read the torque and rotational speed. Trigger and clock signals were sent between each board to start/stop the test and ensure simultaneous data acquisition. In a preliminary study, the sampling rate was set at 62500 Hz to avoid aliasing in the acquired signals.

2.4. Power and efficiency calculation

The electrical power output of the generator, P_{gen}, was calculated using Aron's method. The method calculates the power of a three-phase AC electric machine by measuring the current in two lines and two line-to-line voltages. It is given by

$$P_{\text{gen}} = u_{12} i_1 - u_{23} i_3, \tag{3}$$

where u_{12} and u_{23} are the line-to-line voltages in the three-phase system and i_1 and i_3 are the currents in lines 1 and 3, Fig. 1.

The sum of the voltage and current inaccuracies mainly gives the inaccuracy of the electrical power at the generator terminals. The value of 0.6% is obtained using the calibrated transducers.

After the rotational speed Ω and the generator's counter torque T_{gen} were set, the voltages u_{12} and u_{23} and the currents i_1 and i_3, Fig. 1, were measured. Then the generator's efficiency η_{gen} is calculated using Eq. (2). The inaccuracy of the efficiency is the sum of the electrical and mechanical inaccuracy, $(0.6 + 0.25)\%$. The inaccuracy in the counter torque estimate is then 1.45%, which is acceptable for field testing data and numerical modelling.

In this instrumentation layout, the difference between measured electrical power output and the mechanical power input corresponds to the copper, stray and core electrical losses and the generator's windage and bearings friction mechanical losses.

Although acceptable for input power or torque estimation purposes, higher accuracy is needed for loss calculation purposes, especially for high-efficiency machines. For 5% inaccuracy in loss estimation using the direct method, higher levels of accuracy in measurement instruments should be used [27].

2.5. Filters

Since the purpose is to obtain the electrical power from measurements at the generator's terminals, and the generator is fed by pulse width modulators (PWM) waveforms that give approximately sinusoidal currents, the effect of high harmonics on the current and voltage signals were neglected for efficiency calculation purposes. In this way, only the first harmonics' voltage and current were of interest. Pulse width modulators use voltage pulses with appropriate widths to create almost sinusoidal currents in the electrical machine. This is characterized by nearly sinusoidal currents and voltages, with switching having a first harmonic and other high-frequency harmonics. Since the electrical power is given by the product of voltage per current, only the first harmonics are necessary. To eliminate the high-frequency harmonics in calculating the electrical power, new zero-phase filters were proposed to access the measured variables correctly [28].

The efficiency calculation was based on the correct measurement of torque, rotational speed, currents and phase-to-phase voltages, as well as on the filtering of the signals. A band-pass filter was obtained by sequentially applying a low-pass filter, and a high-pass filter for this purpose.

The low-pass filter was defined by a six-stage Savitzky-Golay (SG) cascade filter whose responses are shown as a function of frequency in Fig. 3a). Fig. 3b) shows that the selection of SG filters with different window lengths n makes it possible to remove the unwanted oscillations in the rejection band of the cascaded filter by exploiting the location of the zeros of the individual filter stages. Since the response of the cascaded filter is defined by the product of the response of the six SG filters, the resulting cascaded filter has a gain in the rejection band several orders of magnitude less than the response of the stage filters. The designed low-pass filter shows a gain of 0.9992 for 50 Hz and drops to 10^{-4} for 200 Hz, see Fig. 3 a).

The high-pass filter is obtained as follows. First, the SG filter depicted in Fig. 4 is applied to the signal. Next, the filter output is subtracted from the original signal to obtain the filtered data. The SG filter of Fig. 4 has a gain of 0.9992 at 3 Hz, which drops to 10^{-4} at 11 Hz.

Fig. 5 depicts the line-to-line voltage u_{12} and the current i_1 in line 1. The raw voltage signal presents the power pulses of the PWM of the VFD to control the voltage and frequency of the generator, see Fig. 5a). It

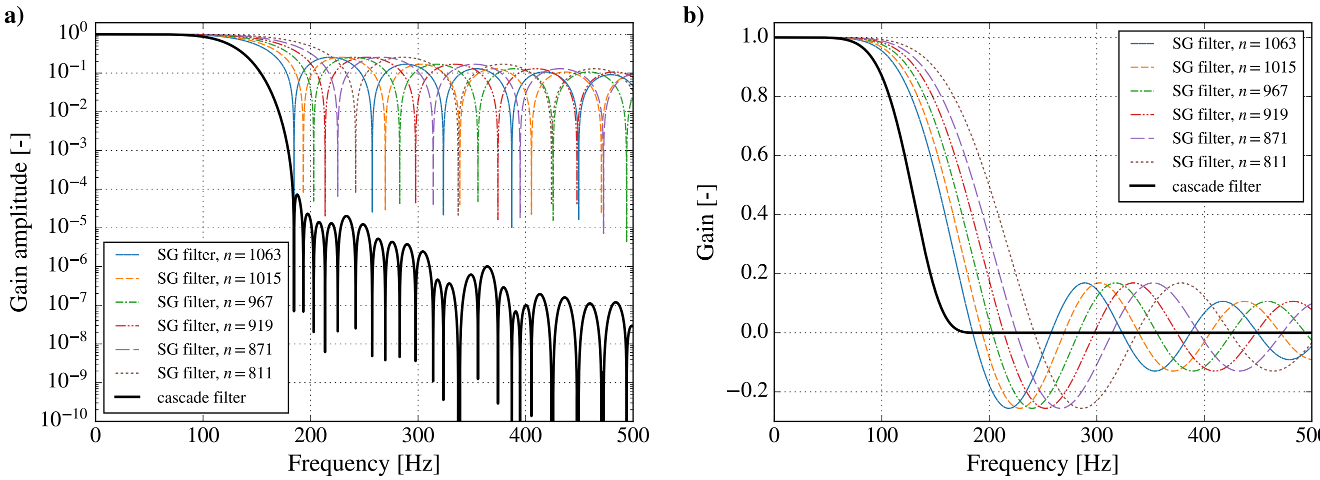

Fig. 3. Savitzky-Golay filters with $n = \{1063, 1015, 967, 919, 871, 811\}$ and the resulting cascade filter for a sampling rate of 62500 Hz. a) semi-logarithmic scale and b) linear scale.

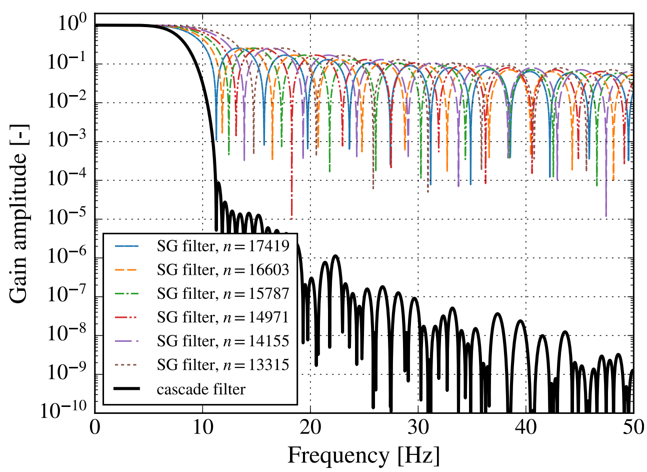

Fig. 4. Savitzky-Golay filters with $n = \{17419, 16603, 15787, 14971, 14155, 13315\}$ and the resulting cascade filter for a sampling rate for 62500 Hz.

consists of a series of voltage pulses to emulate a sine wave. In analysing the filtered voltage signal, this has indeed been achieved. The current signal represented in Fig. 5 b) has a considerable amount of noise that the designed low-pass filter could remove.

3. Results

This section first presents the overall results showing the generator's efficiency for different speeds and loads. These results are helpful for wave energy applications where the rotational speed and generator loads vary significantly in a short time due to wave grouping effects [29] and in a long time due to seasonal variations [23]. It follows the description of the methods for using the data for the two applications: 1) for wave-to-wire numerical modelling of wave energy converters and 2) for post-processing results from experimental campaigns under real sea state conditions. Rational functions are used to approximate the results facilitating further use of the results of this work. Furthermore, they are normalised to the generator's rated power to adapt to other power levels.

Fig. 6 depicts the generator's efficiency as a function of the generator's mechanical power input, $T_{\text{gen}}\Omega$, and the rotational speed, Ω. For a rotational speed range between 700 and 1900 rpm, Fig. 6 shows that the generator's efficiency follows the standard curves for this type of machine. As expected, high efficiency is achieved at relatively low loads. The maximum efficiency is $\eta_{\text{gen}} = 0.92$. At constant load, the efficiency decreases with increasing rotational speed for speeds above 1900 rpm. At rotational speeds below 400 rpm, the current and voltage values are very low and inaccurate due to the sensors used. They have been excluded from this analysis.

For application in numerical wave-to-wire models, the efficiency of the generator can be expressed as a function of the mechanical input power, normalised to the rated power of the generator, $T_{\text{gen}}\Omega/P_{\text{gen}}^{\text{rated}}$, and the rotational speed, Ω, using the experimental data fitting by the

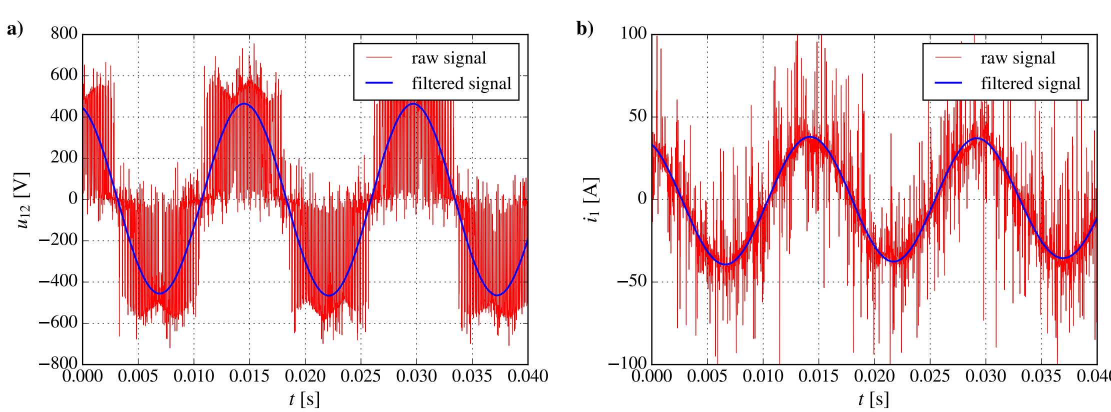

Fig. 5. a) Raw (red) and filtered (blue) signals of voltage between lines 1 and 2 and b) current in line 3, for rotational speed $\Omega = 1993$ rpm and $P_{\text{gen}} = 11.9$ kVA.

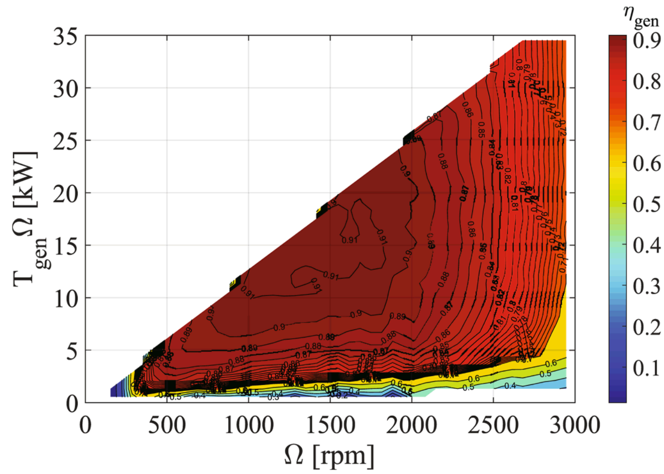

Fig. 6. Generator's efficiency as a function of the input mechanical power and rotational speed.

Table 2
List of the coefficients for Eq. (4).

j	Ω [rpm]	a_{0j}	a_{1j}	a_{2j}	b_j	R^2
1	[400, 2100]	−0.008211	0.947866	−0.047832	0.000202	0.9724
2	2200	−0.014040	0.921300	−0.034090	−0.003214	0.9999
3	2300	−0.010510	0.912600	−0.036910	0.001371	0.9997
4	2400	−0.013710	0.903400	−0.037830	0.000279	1.0000
5	2500	−0.012800	0.895800	−0.042710	0.004842	0.9999
6	2600	−0.017370	0.876500	−0.042290	0.001866	0.9998
7	2700	−0.014000	0.846700	−0.037160	0.003523	0.9999
8	2800	−0.016520	0.803900	−0.025730	−0.001978	1.0000
9	2900	−0.015070	0.774100	−0.027590	0.004074	0.9999
10	2980	−0.015210	0.740500	−0.023310	0.004324	1.0000

rational polynomial function

$$\eta_{gen}\left(\frac{T_{gen}\Omega}{P_{gen}^{rated}},\Omega\right)=\frac{\sum_{k=0}^{2}a_{k,j}\left(\frac{T_{gen}\Omega}{P_{gen}^{rated}}\right)^k}{\frac{T_{gen}\Omega}{P_{gen}^{rated}}+b_j}, \tag{4}$$

where the coefficients $a_{k,j}$ and b_j are listed in Table 2 as a function of the rotational speed Ω. The R-square coefficient of determination presents a minimum value of $R^2 = 0.9724$. From Fig. 7, it can be seen that the

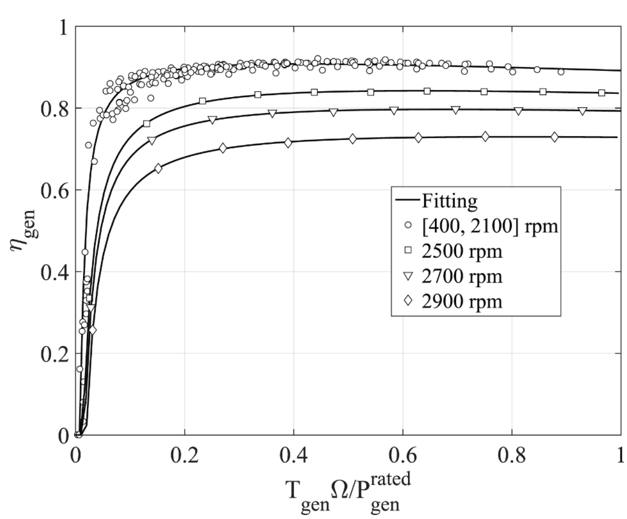

Fig. 7. Fitting of experimental data, as given by Eq. (4), for selected rotational speeds.

Table 3
List of the coefficients for Eq. (5).

j	Ω [rpm]	c_{0j}	c_{1j}	c_{2j}	d_j	R^2
1	[400, 2100]	0.000480	0.940900	−0.037260	0.007993	0.9891
2	2200	0.000832	0.922500	−0.039990	0.010560	0.9999
3	2300	0.000478	0.912700	−0.042630	0.012270	0.9997
4	2400	0.000123	0.903700	−0.044580	0.014170	1.0000
5	2500	0.001221	0.894900	−0.050120	0.018050	0.9999
6	2600	0.000382	0.876200	−0.051560	0.019310	0.9999
7	2700	0.000803	0.846300	−0.046530	0.017680	0.9999
8	2800	0.000316	0.804700	−0.034370	0.014840	0.9999
9	2900	0.000674	0.773200	−0.037110	0.018730	0.9999
10	2980	0.000624	0.739500	−0.032310	0.018830	1.0000

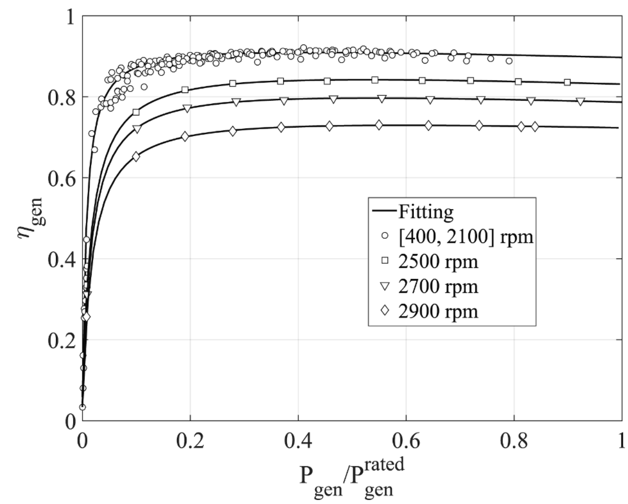

Fig. 8. Fitting of experimental data, as given by Eq. (5), for selected rotational speeds.

curve fitting expressed by Eq. (4) shows good agreement with the experimental values, as expected given the value of R^2.

In post-processing routines of experimental data of turbine generator prototypes, the efficiency of the generator as a function of the load, P_{gen}/P_{gen}^{rated}, and the rotational speed, Ω, may be approximated by a rational polynomial function

$$\eta_{gen}\left(\frac{P_{gen}}{P_{gen}^{rated}},\Omega\right)=\frac{\sum_{k=0}^{2}c_{k,j}\left(\frac{P_{gen}}{P_{gen}^{rated}}\right)^k}{\frac{P_{gen}}{P_{gen}^{rated}}+d_j}, \tag{5}$$

where the coefficients $c_{k,j}$ and d_j are listed in Table 3 as a function of the rotational speed, Ω. The R-square coefficient of determination presents a minimum value of $R^2 = 0.9891$. From Fig. 8, it can be seen that the curve fitting by Eq. (5) shows good agreement with the experimental values, as expected from the R^2 values.

The coefficients of the rational polynomial functions found for each data set were determined using the Curve Fitting toolbox of MATLAB 2022b.

4. Conclusion

As with any emerging technology, the initial deployment of prototypes primarily focuses on ensuring the functioning of the entire system, consolidating operation and maintenance strategies, and analysing the details that have been missed. Careful analysis of all the data from the test campaigns for these prototypes is of utmost importance, using the most accurate data possible. The complete characterisation of the energy chain, from the kinetic and potential energy from the waves to the electric power injected into the grid, is a requirement of the wave energy industry.

The robustness of numerical models simulating oscillating water columns (wave-to-wire models) and the post-processing of experimental data from prototypes depend heavily on the generator's efficiency that equips this wave energy converter. This paper discusses the method for both situations based on the experimental characterisation of a 30 kVA induction generator. A new filter was designed to allow the correct post-processing of the raw data from the current experiment.

Results show that under different load conditions and rotational speeds, the typical curve of these electric machines is considerably different from the single curve usually adopted when oscillating water column devices are simulated. Because the turbine-generator rotational speed is easily measured with high accuracy, the torque estimation accuracy obtained using this methodology is mainly determined by the mechanical power inaccuracy, given by the generator power and efficiency inaccuracies.

This study is essential for the numerical simulation and field testing of oscillating-water-column wave energy converters with the presentation of detailed data for different rotational speeds and loads of a squirrel cage asynchronous electrical generator connected to a four-quadrant variable frequency drive. The results are normalised to the generator's rated power, allowing quick adaptation to the user's needs.

CRediT authorship contribution statement

A.A.D. Carrelhas: Data curation, Investigation, Methodology, Software, Validation, Formal analysis, Visualization, Writing – original draft. **L.M.C. Gato:** Conceptualization, Investigation, Methodology, Validation, Formal analysis, Supervision, Resources, Funding acquisition, Writing – original draft. **J.C.C. Henriques:** Conceptualization, Software, Supervision, Writing – review & editing. **G.D. Marques:** Formal analysis, Methodology, Validation, Writing – review & editing.

Declaration of Competing Interest

The authors declare that they have no known competing financial interests or personal relationships that could have appeared to influence the work reported in this paper.

Data availability

Data will be made available on request.

Acknowledgement

This research was partially supported by European Union's Horizon 2020 Research and Innovation Programme under Grant Agreement No. 654444 (OPERA Project) and the Portuguese Foundation for Science and Technology - FCT, through IDMEC, under LAETA, Project UIDB/50022/2020 and INESC-ID Project UIDB/50021/2020.

References

[1] Dall-Orsoletta A, Ferreira P, Gilson Dranka G. Low-carbon technologies and just energy transition: Prospects for electric vehicles. Energy Conversion Manage 2022; X 16:100271. https://doi.org/10.1016/j.ecmx.2022.100271.

[2] Dastan SA, Selcuk O. Review of the security of supply in Turkish energy markets: Lessons from the winter shortages. Renew Sustainable Energy Rev 2016;59:958–71. https://doi.org/10.1016/j.rser.2016.01.015.

[3] Novo R, Marocco P, Giorgi G, Lanzini A, Santarelli M, Mattiazzo G. Planning the decarbonisation of energy systems: The importance of applying time series clustering to long-term models. Energy Conversion Manage: X 2022;15:100274. https://doi.org/10.1016/j.ecmx.2022.100274.

[4] Das TK, Kerikous E, Venkatesan N, Janiga G, Thévenin D, Samad A. Performance improvement of a Wells turbine through an automated optimization technique. Energy Conversion Manage: X 2022;16:100285. https://doi.org/10.1016/j.ecmx.2022.100285.

[5] Said HA, Garcia-Violini D, Ringwood JV. Wave-to-grid (W2G) control of a wave energy converter. Energy Conversion Manage: X 2022;14:100190. https://doi.org/10.1016/j.ecmx.2022.100190.

[6] Tedd J, Kofoed JP. Measurements of overtopping flow time series on the Wave Dragon wave energy converter. Renew Energy 2009;34:711–7. https://doi.org/10.1016/j.renene.2008.04.036.

[7] Carrelhas AAD, Gato LMC, Falcão AFO, Henriques JCC. Control law design for the air-turbine generator set of a fully submerged 1.5 MW mWave prototype. Part 1: Numerical modelling. Renew Energy 2022;181:1402–18. https://doi.org/10.1016/j.renene.2021.09.011.

[8] Falcão AFO. Wave energy utilization: A review of the technologies. Renew Sustainable Energy Rev 2010;14(3):899–918. https://doi.org/10.1016/j.rser.2009.11.003.

[9] Falcão AFO, Sarmento AJNA, Gato LMC, Brito-Melo A. The Pico OWC wave power plant: Its lifetime from conception to closure 1986–2018. Appl Ocean Res 2020;98:102104. https://doi.org/10.1016/j.apor.2020.102104.

[10] Heath T, Chapter 334 - The development and installation of the Limpet wave energy converter, in: A. Sayigh (Ed.), World Renewable Energy Congress VI, Pergamon, Oxford, 2000, pp. 1619 – 1622. doi:10.1016/B978-008043865-8/50334-2.

[11] Torre-Enciso Y, Ortubia I, López de Aguileta LI, Marqués J, Mutriku Wave Power Plant: From the thinking out to the reality, in: Proc 8th European Wave Tidal Energy Conf, Uppsala, Sweden, 2009, pp. 319–329.

[12] Weller S, Parish D, Gordelier T, de Miguel Para B, Garcia E, Goodwin P, et al., Open sea OWC motions and mooring loads monitoring at BiMEP, in: Proc 12th European Wave Tidal Energy Conf, Cork, Ireland, 2017.

[13] OE 35 Buoy, Ocean Energy, A World of Power, https://oceanenergy.ie/oe35/, Accessed: April 2023.

[14] Wave Swell - UniWave200 - King Island project, https://www.waveswell.com/, Accessed: April 2023.

[15] Carrelhas AAD, Gato LMC, Henriques JCC, Falcão AFO. Experimental study of a self-rectifying biradial air turbine with fixed guide-vanes arranged into two concentric annular rows. Energy 2020;198:117211. https://doi.org/10.1016/j.energy.2020.117211.

[16] OPERA - Open Sea Operating Experience to Reduce Wave Energy Cost, Contract 654444, http://opera-h2020.eu/, Accessed: April 2023.

[17] Portillo JCC, Collins KM, Gomes RPF, Henriques JCC, Gato LMC, Howey BD, Hann MR, Greaves DM, Falcão AFO. Wave energy converter physical model design and testing: The case of floating oscillating-water-columns. Appl Energy 2020;278:115638. https://doi.org/10.1016/j.apenergy.2020.115638.

[18] Faÿ F-X, Henriques JCC, Kelly J, Mueller M, Abusara M, Sheng W, Marcos M. Comparative assessment of control strategies for the biradial turbine in the Mutriku OWC plant. Renew Energy 2020;146:2766–84. https://doi.org/10.1016/j.renene.2019.08.074.

[19] Kelly JF, Wright WMD, Sheng W, Sullivan KO. Implementation and verification of a wave-to-wire model of an oscillating water column with impulse turbine. IEEE Trans Sustainable Energy 2016;7(2):546–53. https://doi.org/10.1109/TSTE.2015.2504463.

[20] Otaola E, Garrido AJ, Garrido I, Lekube J, Liria P, Mader J, Development and validation of an OWC capture chamber model by means of measured experimental data, in: 5th International Conference on Instrumentation and Measurement, Computer, Communication and Control (IMCCC), 2015, pp. 488–492. https://doi.org/10.1109/IMCCC.2015.109.

[21] Benreguig P, Kelly JF, Pakrashi V, Murphy J, Wave-to-wire model development and validation for two OWC type wave energy converters, Energies 2019 (20). https://doi.org/10.3390/en12203977.

[22] Henriques JCC, Portillo JCC, Gato LMC, Gomes RPF, Ferreira DN, Falcão AFO. Design of oscillating-water-column wave energy converters with an application to self-powered sensor buoys. Energy 2016;112:852–67. https://doi.org/10.1016/j.energy.2016.06.054.

[23] Ciappi L, Simonetti I, Bianchini A, Cappietti L, Manfrida G. Application of integrated wave-to-wire modelling for the preliminary design of oscillating water column systems for installations in moderate wave climates. Renewable Energy 2022;194:232–48. https://doi.org/10.1016/j.renene.2022.05.015.

[24] Vas P. Sensorless Vector and Direct Torque Control. Oxford University Press; 1998. https://doi.org/10.1017/CBO9780511754630.

[25] Sender M, Wallscheid O, Böcker J. Accurate torque control for induction motors by utilizing a globally optimized flux observer. IEEE Trans Power Electron 2021;36:13261. https://doi.org/10.1109/TPEL.2021.3080129.

[26] Gato LMC, Henriques JCC, Carrelhas AAD. Sea trial results of the biradial and Wells turbines at Mutriku wave power plant. Energy Conversion Manage 2022;268:115936. https://doi.org/10.1016/j.enconman.2022.115936.

[27] Aarniovuori MNL, Karkkäinen H, Pyrhönen J, Measurement accuracy requirements for the efficiency classification of converters and motors, in: 21st European Conference on Power Electronics and Applications (EPE '19 ECCE Europe), 2019, pp. 1–10. doi:10.23919/EPE.2019.8915560.

[28] André JMCS, Savitzky-Golay cascade filter design, IST Technical Report, 2021.

[29] Carrelhas AAD, Gato LMC. Reliable control of turbine-generator set for oscillating-water-column wave energy converters: Numerical modelling and field data comparison. Energy Conversion Manage 2023;282:116811. https://doi.org/10.1016/j.enconman.2023.116811.